DEUTSCHES ELEKTRONEN – SYNCHROTRON DESY

DESY 89-157
November 1989

Wide Band Multi-Bunch Feedback Systems for PETRA

D. Heins, J. Klute, R. D. Kohaupt, K.-H. Matthiesen,
S. Pätzold, J. Rümmler, M. Schweiger

Deutsches Elektronen-Synchrotron DESY, Hamburg

ISSN 0418-9833

NOTKESTRASSE 85 · 2 HAMBURG 52

To be sure that your preprints are promptly included in the
HIGH ENERGY PHYSICS INDEX,
send them to the following address (if possible by air mail):

DESY
Bibliothek
Notkestrasse 85
2 Hamburg 52
Germany

DESY 89-157
November 1989

ISSN 0418-9833

Wide band multi-bunch feedback systems for PETRA

D. Heins, J. Klute, R. D. Kohaupt, K.-H. Matthiesen, S. Pätzold,
J. Rümmler, M. Schweiger
presented by R. D. Kohaupt

November 28, 1989

1 Introduction:

The central intensity limitation for the PETRA- and HERA e^--rings is connected with the coupled bunch motion.

The multi-bunch instabilities are driven by the parasitic modes of the accelerating cavities, thus limiting the total current. The threshold currents in PETRA were computed (1,2) at around 10 mA. The actual transverse thresholds were observed to be at 7 mA.

In HERA the computed threshold currents are below 10 mA and the observed thresholds turned not to be at 3 mA. The bunch spacing in PETRA and HERA is the same

$$\Delta t = 96\, nsec$$

Therefore the number of bunches in PETRA is 80 and in HERA this number is 220. In order to get rid of the severe current limitation we decided to damp the multi-bunch instabilities with help of wide band transverse and longitudinal multi-bunch feedback systems. These systems will be the same for both machines. In the mean time the transverse feedback systems for PETRA have been brought into operation and successfully tested.

All horizontal and vertical beam modes were damped. The damping rate achieved was below 200 μsec in comparison with the natural decay time (Landau damping) of 10 msec. The total current reached was 43 mA, limited mainly by the increasing vacuum pressure induced by the sudden high current. The first onset of longitudinal instabilities was observed.

2 The feedback system

The feedback systems are nearly identical in the horizontal and vertical directions. The block diagram of the whole system (hor. and vert.) is shown in fig. 1. A four-button orbit monitor serves as the horizontal and vertical pick-up station.

After filtering at 100 MHz with a bandwidth of 30 MHz the signal is pre-amplified, split and recombined for the horizontal and vertical plane. The amplitude modulated rf is then transfered to a pair of rf signals with an amplitude dependent relative phase modulation at the output of a 90°-hybrid. After passing a limiter amplifier of 50 dB gain the phase demodulation is performed at a phase detector.

Due to this scheme a high signal-to-noise ratio was reached leading to a resolution of 1/10 mm at a single bunch current of 20 μA. At the output of the pick-up electronics the signal of transverse displacements produced by the single bunches of the beam is available for digitalization. Before that is done the signal will be amplified by an adjustable "range" amplifier in order to adjust the analog output to the input of the digital component of the system. The 8-bit ADC is triggered by the PETRA trigger system (PIT).

The digital filter is the central unit for signal processing. Here the proper bucket delay is adjusted which is necessary for the correct coincidence of signal- and bunch-arrival at the kickers. The setting of the phase for damping is achieved by a phase shifter built up as a digital FIR filter. After filtering, the digital data are transferred to the digital modulator which shifts the baseband of 10 kHz to 5 MHz to a frequency range of 5 MHz to 10 MHz which is the operational range for the combination of the kicker and the power amplifier. The digital data is transferred back to the analog level by a 10-Bit DAC.

The regeneration filter is built up as a 7th order Butterworth low pass filter. The output can be delayed within 96 nsec with an accuracy of 1 nsec for fine tuning of the delay. After passing an adjustable "gain" amplifier the power amplifier is driven. This amplifier delivers a maximum power of 1 kW between 5 MHz and 10 MHz. The output of this amplifier finally feeds the delay-line deflection kicker.

3 Theoretical back ground

The bunch system can be described in a rather simplified way by

$$(\Omega^2 - Z^2)\tilde{X}_\mu = \sum_{\nu=0}^{N-1} A_{\mu\nu}(Z)\tilde{X}_\nu,\ \mu = 0 \ldots N-1 \tag{1}$$

where the $\tilde{X}\mu$ denote the transverse displacements of the bunch in the Fourier-Laplace representation Ω, Z are the unperturbed and complex frequencies of the system. The matrix $A_{\mu\nu}(Z)$ is the feedback matrix containing all transfer functions of the system.

For an ideal bunch-to-bunch feedback system the matrix $A\mu\nu$ is a multiple of the unit matrix:

$$A_{\mu\nu} = A(Z) \cdot \delta_{\mu\nu} \tag{2}$$

However, due to the fact that the analog components deviate from an ideal frequency response, a perfect bunch-to-bunch feedback system cannot be realized. Therefore the matrix $A_{\mu\nu}$ must be written as

$$A_{\mu\nu} = \tilde{T}(Z) \cdot \sum_{r=0}^{N-1} K_{\mu r}\tilde{G}_r K^*_{\nu r} \tag{3}$$

where the $K_{\mu r}$ are the components of the normal mode vectors

$$\vec{K}_r = \frac{1}{\sqrt{N}} \left\{ \begin{array}{c} \vdots \\ e^{2\pi i\nu r/N} \\ \vdots \end{array} \right\} \leftarrow \nu, r = 0, \cdot\cdot N-1 \tag{4}$$

The function $\tilde{T}(Z)$ describes the properties of the FIR filter which acts on the different bunches separately. The quantity $\tilde{G}_r$ is the overall transfer function of the analog system. This function is defined as:

$$G_r = \tilde{G}(\Omega_r),\ with\, \Omega_r = r\omega_c, \tag{5}$$

ω_c being the circular revolution frequency. Therefore this function can be directly determined by measuring the frequency response of the analog components of the system.

In order to find out what is the influence of a non-ideal frequency response on the damping efficiency of the system we transform equ. (1) into the "normal mode" representation. This yields:

$$(\Omega^2/Z^2)C_r = \tilde{T}(Z)\tilde{G}(\Omega_r) \cdot C_r,\ r = O, \ldots, N-1 \tag{6}$$

where C_τ denote the mode coefficents. In this representation the system becomes diagonal. We have to look for the solutions

$$(\Omega^2 - Z^2) - \tilde{T}(Z)\tilde{G}(\Omega_\tau) = 0 \tag{7}$$

The transfer function $\tilde{G}(\Omega)$ can be rewritten as

$$\tilde{G}(\Omega) = \mid \tilde{G}(\Omega) \mid e^{i\chi(\Omega)}, \tag{8}$$

and the frequency response can be described by the amplitude response $\mid \tilde{G}(\Omega) \mid$ and the phase response $\chi(\Omega)$. Any phase response can be represented in the form

$$\chi(\Omega) = \tau\Omega + \Delta\chi(\Omega), \tag{9}$$

where $\tau\Omega$ is a linear "average" part. Since such a part represents a delay we can drop this part because the total delay of the system must be completed to a full turn in order to accomplish the coincidence of signal and bunch arrival at the kicker. Therefore we obtain instead of (7)

$$(\Omega^2 - Z^2) - \mid \tilde{T}(Z) \mid e^{i\varphi} . \mid \tilde{G}(\Omega_\tau \mid e^{i\Delta\chi(\Omega_\tau)} \tag{10}$$

In order to obtain maximum damping for all beam modes we have to keep $\mid \tilde{G}(\Omega) \mid$ constant and $\Delta\chi$ small. The phase φ has to be properly adjusted.

4 The components

4.1 The pick-up electronics

Fig. 2 shows the block diagram of the pick-up electronics. This system operates at 100 MHz with a bandwidth of about 30 MHz. The closed orbit deviations of the beam are compensated by controlling the electrical offset by a single bunch signal after passing a low pass filter cutting the betatron oscillations.

4.2 The digital filter (DIFI)

Fig. 3 shows the delay condition for a rotating bunch. The total natural delay of the system is denoted by T_E, and τ is the delay which has to be added by the digital filter for completing a full turn. The phase shifter has been built up as a digital FIR filter according to

$$g_\mu = \sum_{k=0}^{2} T_k f_{\mu-k} \tag{11}$$

where f and g are input and output data respectively. The coefficients determine the filter, taking

$$T_0 = \frac{2}{\pi} sin\varphi,\ T_1 = cos\varphi,\ T_2 = -\frac{2}{\pi} sin\varphi, \tag{12}$$

the transfer function in the frequency domain gives

$$\tilde{T}(\delta Q) = \left\{ cos\varphi + \frac{4}{\pi} i sin 2\pi\delta Q \cdot sin\varphi \right\} e^{-2\pi i \delta Q} \tag{13}$$

δQ being the fractional part of the transverse time. Apart from the delay factor $e^{-2\pi i\delta Q}$ the quantity $\tilde{T}(\delta Q)$ behaves as a phase shifter in the variable φ within the range $0.1 \leq \delta Q \leq 0.4$. The advantage of this 3-coefficient-FIR-filter is the fast processing.

Fig. 4 shows the DIFI block diagram. The shift registers serve to set the bucket delay and provide the locations for the signals of the proceeding turns according to equ. (12). The coefficients h are stored in the coefficient "ROMs".

Each bunch is treated separately but identically within the bunch spacing of 96 nsec. Therefore only one phase shifter is needed, which simplifies the adjustment considerably.

4.3 The digital modulator and the regeneration filter

In order to shift the base band of transverse displacements to the frequency range between 5 MHz to 10 MHz a digital modulator has been applied. Fig. 5 shows the principle idea. Instead of using only a single digital word within the sampling time T_B (fig. 5a) the modulator produces an inverted word behind each original digital word. At the output of the DAC and after passing the regeneration filters one obtains a 10 MHz signal instead of the dc-component. Accordingly the base band is shifted into the range between 5 MHz to 10 MHz.

4.4 The power amplifier(s)

The power amplifier is of class A type and has a maximum power output of 1 kW within the frequency range between 200 kHz to 35 MHz.

4.5 The kicker(s)

The deflection kickers are built up as ferrite-capacitor-loaded 10 cell delay lines. The schematic of a single cell of the horizontal kicker is shown in

Fig. 6a. In order to protect the ferrite material against the beam induced voltage we use a strip chamber within the kicker (fig. 6a and fig. 6b). Great effort was made to linearize the amplitude and phase response of the kickers.

5 Measurements

The amplitude and phase response was measured for each component, separately and in combination with all components of the loop. The transfer function of the cable connection between the power amplifier and the kicker in the rings was studied theoretically in order to determine the tolerances for the input impedance of the kicker in the range between 5 MHz and 10 MHz. This function was checked experimentally by measuring the frequency response between the PA input and the kicker output (absorber) after installation in the ring.

For the complete system the deviation from constant amplitude response was found to be less than 0.5 dB. The deviation from ideal phase response was less than $\pm 15°$. The influence of phase deviation on the damping efficiency is 6 % for a phase deviation of $\pm 20°$.

6 Adjustment of the system

The adjustment of the feedback system was performed according to the following scheme:

1. Injection of a single bunch.
2. Converter timing and bucket adjustment by setting the delay.
3. Ecitation of horizontal and vertical oscillations by horizontal (injection) and vertical (diagnostic) kickers.
4. Adjustment of phase and fine delay for maximum damping.
5. Injection of a multi-bunch filling of 70 bunches (80 locations with a gap of 10 locations) with spacing of 96 nsec.
6. Ecitation of all horizontal and vertical normal modes with help of a noise-modulated rf generator feeding the feedback power amplifier.
7. Time tune of phase adjustment for overall mode damping.

7 Results

Without feedback damping, the damping time in PETRA is determined by the filamentation time ("Landau decay" time) and this is shown in fig. 7. A single bunch was excited by the horizontal injection kickers. The coherent damping time is about 10 msec. Fig. 8 shows the behaviour of the beam on the same scale when the feedback loop has been closed. Fig. 9 shows the same behaviour for a higher time resolution. The observed coherent damping time is about 300 μsec. When the full gain was applied, the damping decreased to values around 100 μsec (Fig. 10). When a multi-bunch filling was injected, the beam remained completely stable in the transverse direction up to 43 mA total current. Above 35 mA we could observe spurious signals due to the first onset of longitudinal coupled bunch instabilities. But even at 43 mA this did not lead to a limitation of the current. The limitation was mainly due to a strong outgassing induced by the sudden high current. Therefore the vacuum pressure increased and as a consequence the lifetime was rapidly reduced.

The injection efficiency was increased even at high currents, which is a consequence of the extreme damping time even at the maximum current.

8 Longitudinal feedback system

The pick-up system, the phase detection system and the digital filters have been successfully tested, damping a single bunch via the main cavities. The complete system, which includes an 1 GHz rf station providing a maximum voltage of 50 kV within a bandwidth of 5 MHz, will be tested at PETRA in 1990.

9 Conclusion

The transverse feedback systems have been successfully tested in PETRA. Therefore work has started to bring these systems to the final version, and activities have already started to copy these systems for HERA. This also includes the longitudinal feedback system.

The description and the tests of the longitudinal feedback system will be published as soon as possible.

10 References

(1) R.D. Kohaupt, DESY-Report M-85-07

(2) K. Balewski, R.D. Kohaupt, DESY-Report to be published

11 Acknowledgement

The authors are grateful to Dr. H.-J. Stuckenberg for his continous help in the field of digital filters, and to S. G. Wipf for reading the manuscript.

12 Figure Captions

1. Block diagram for the transverse feedback system (MBFB).
2. Block diagram of the transverse deflection system.
3. Delay conditions for a rotating bunch.
4. Block diagram of the digital filter.
5. Digital modulator and L.P. filter.
6. Schematic of the transverse kicker.
7. Beam damping, feedback loop open.
8. Beam damping, feedback loop closed.
9. Beam damping, feedback loop closed.
10. Beam damping, feedback loop closed maximum gain.

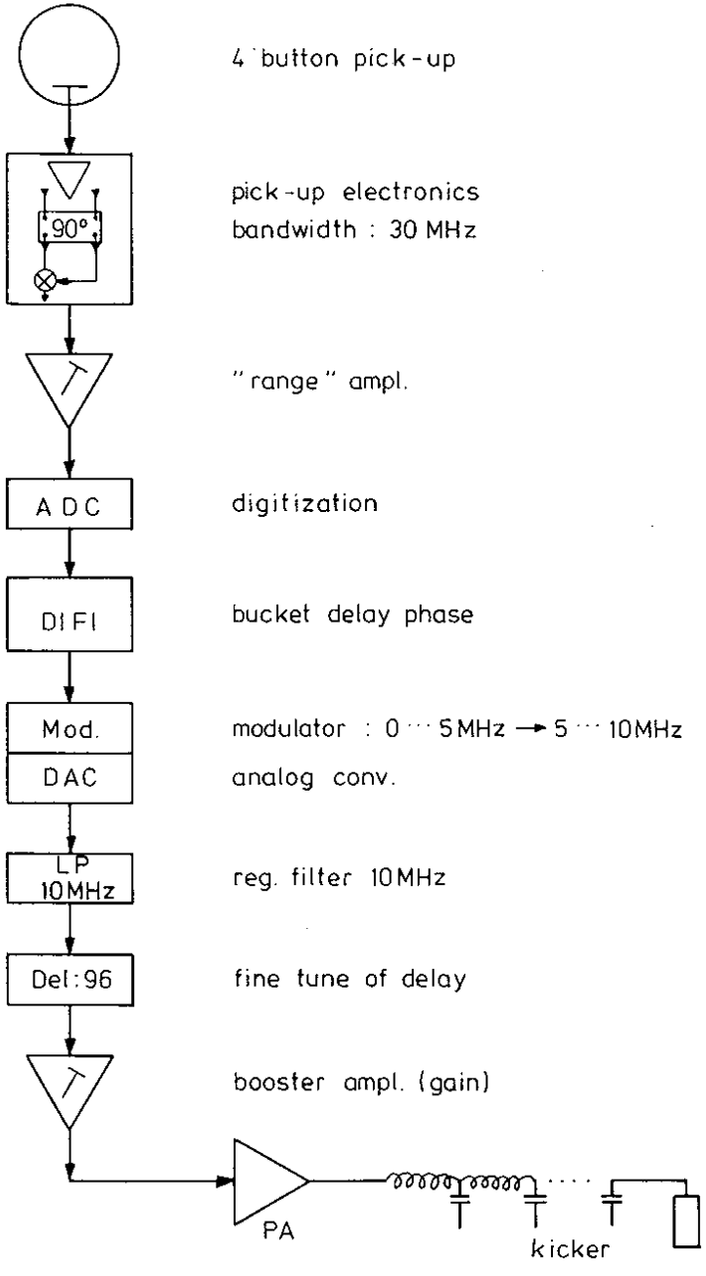

Fig. 1 block diagram of the transverse MBFB

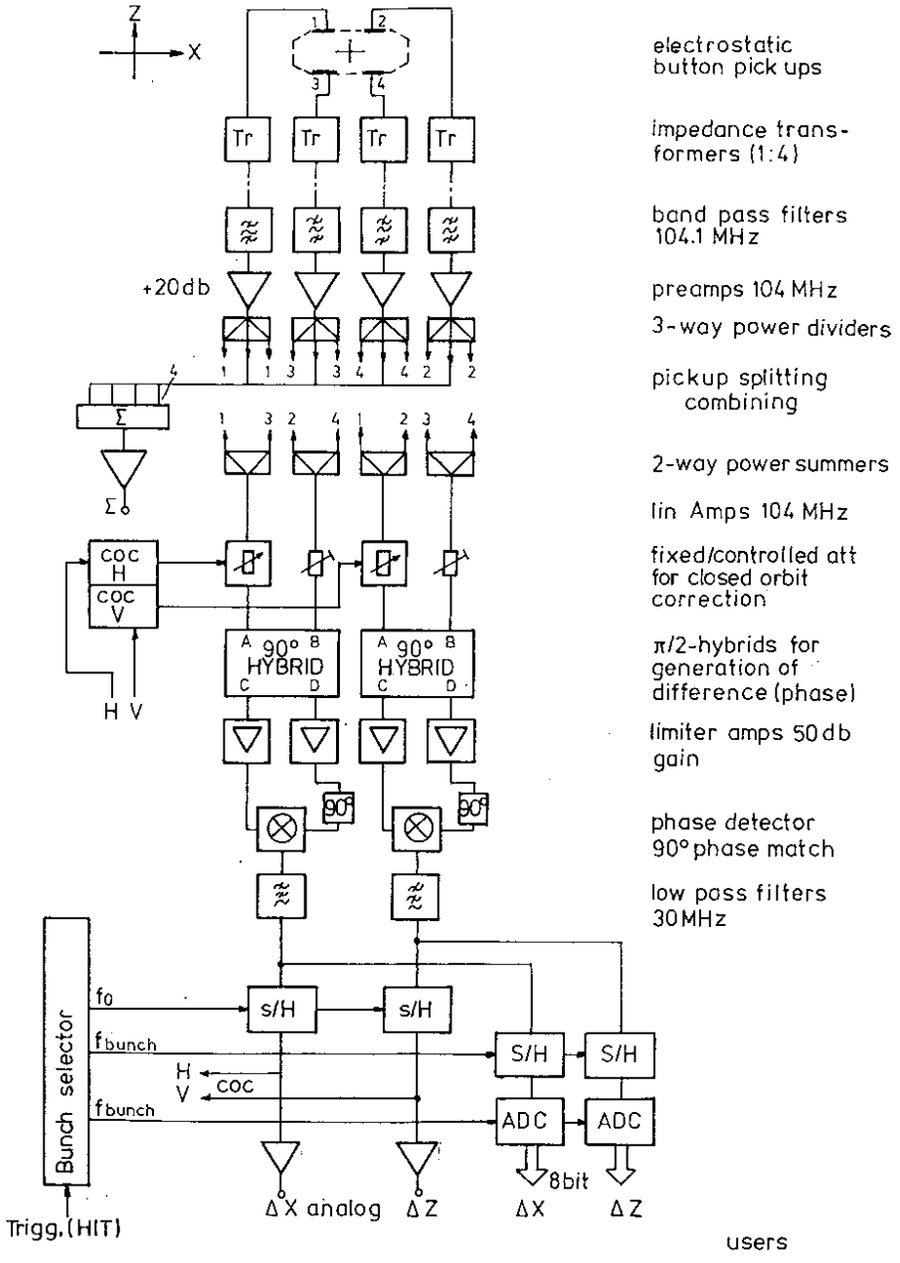

Fig. 2 block diagram of transverse detector

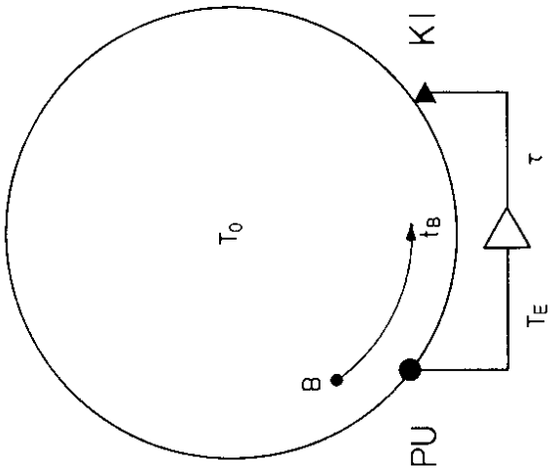

$T_E = nT_0 + t_E \,,\; t_E > t_B$

condition for coincidence of signal and bunch arrival

$t_B + m \cdot T_0 = nT_0 + t_E + \tau$

$\tau = (m-n)T_0 - (t_E - t_B)$

Min $(\tau) \geq 0$

$\tau = T_0 - (t_E - t_B) \longrightarrow \underline{\tau = T_0 - d}$

Fig. 3 delay conditions for the feedback system

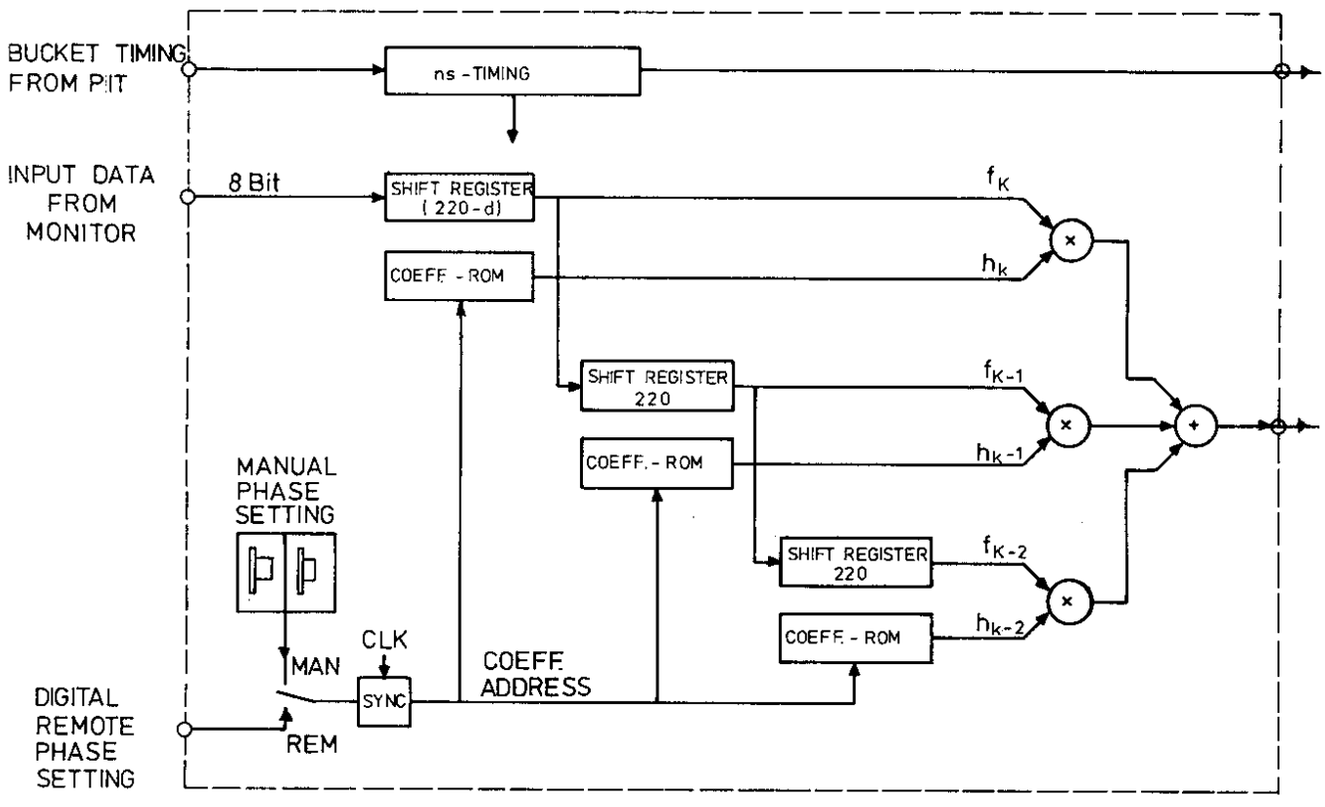

d = external delay , measured in buckets

Fig. 4 DIGITAL FILTER

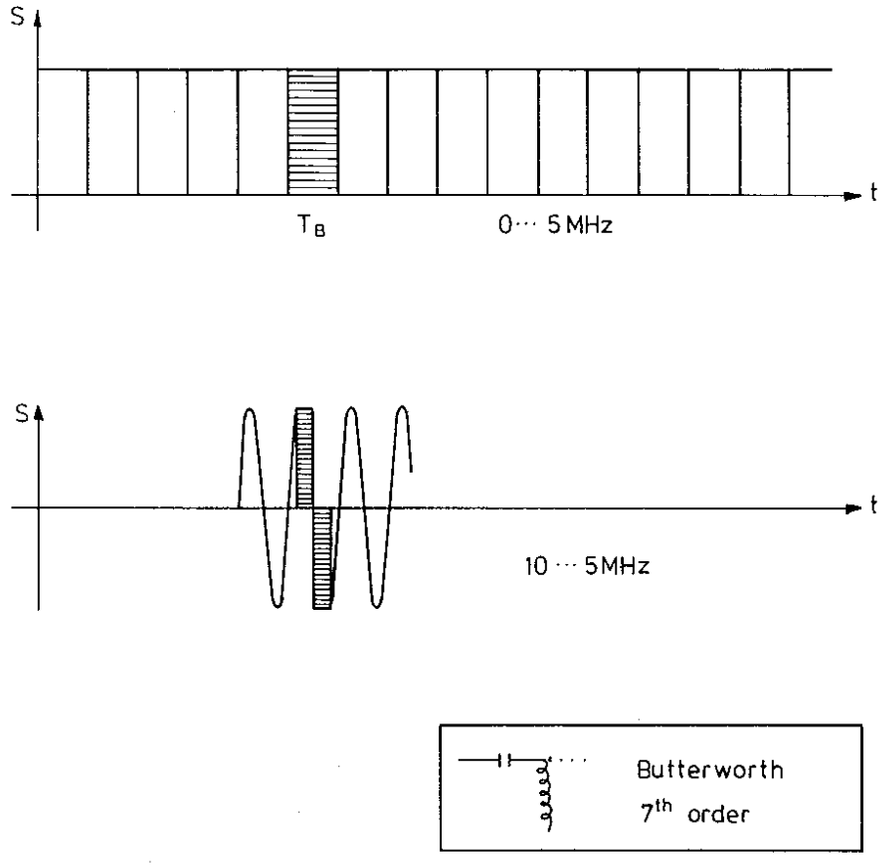

Fig. 5 Digital modulator and L.P. filter

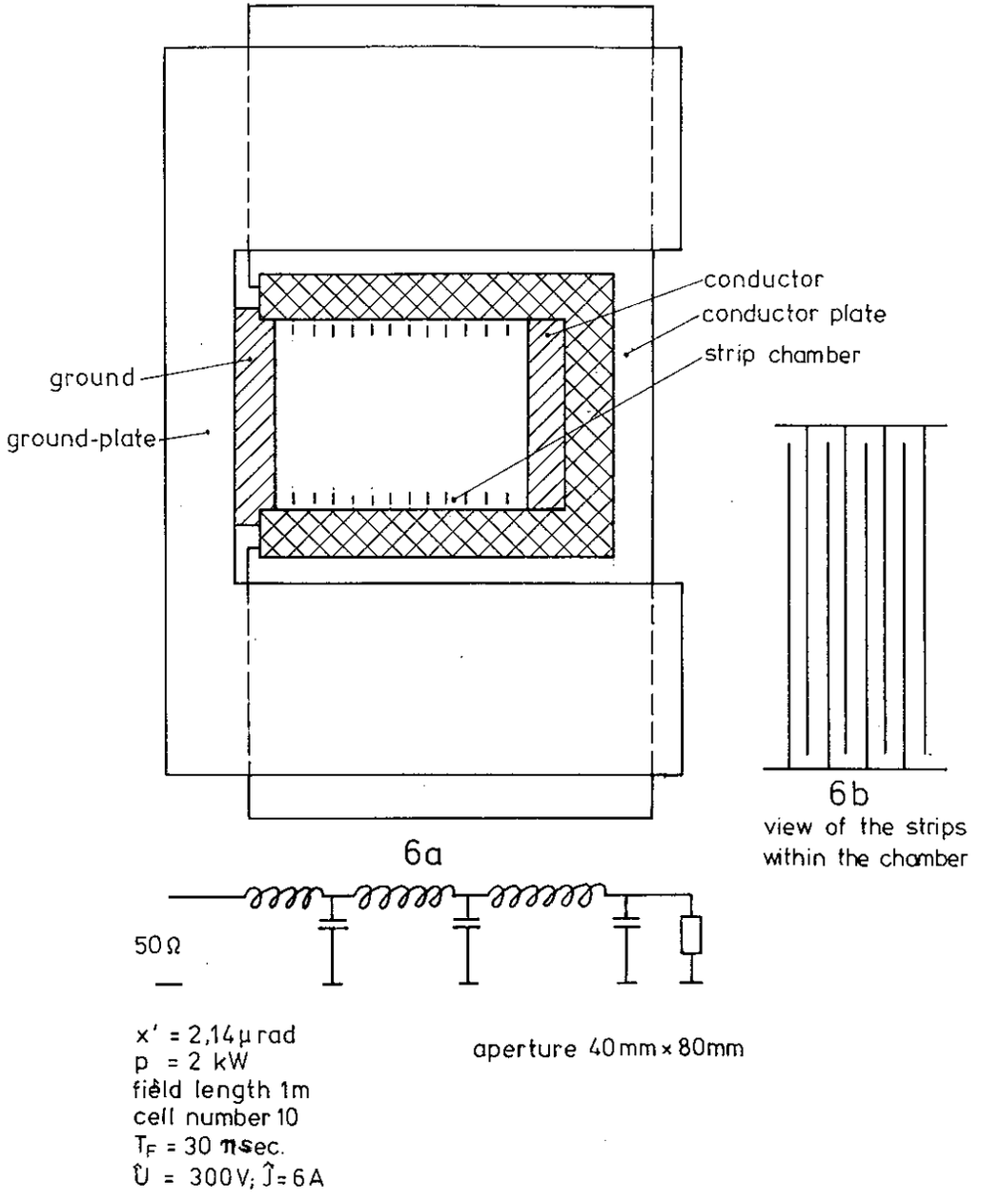

Fig. 6 schematic of horizontal kicker and strip chamber

08: 42: 22 86 Dec 05

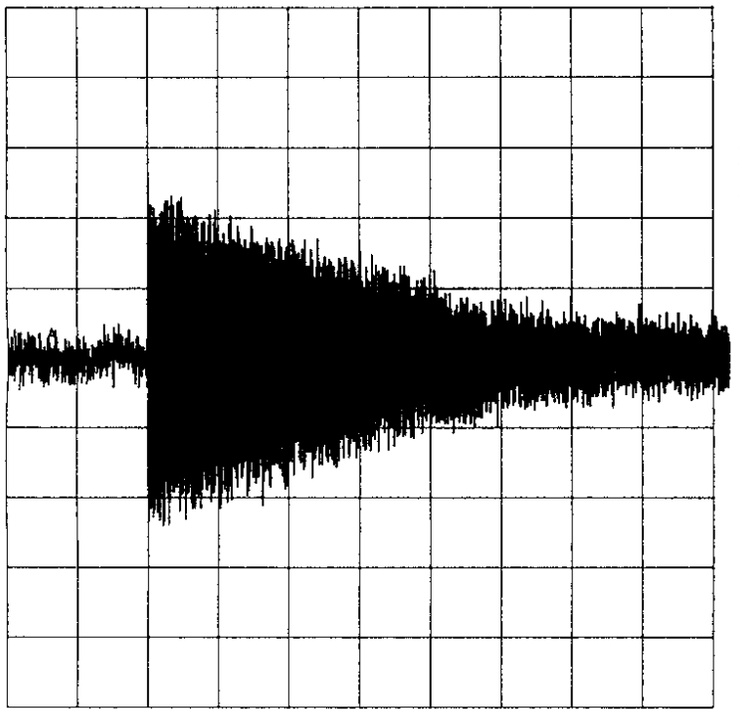

. REGO A: 1 V T: 2ms REC AC
. B: 200mV D: - 2DIV / A

Fig. 7 beam damping, feedback loop open

10: 04: 49 86 Dec 05

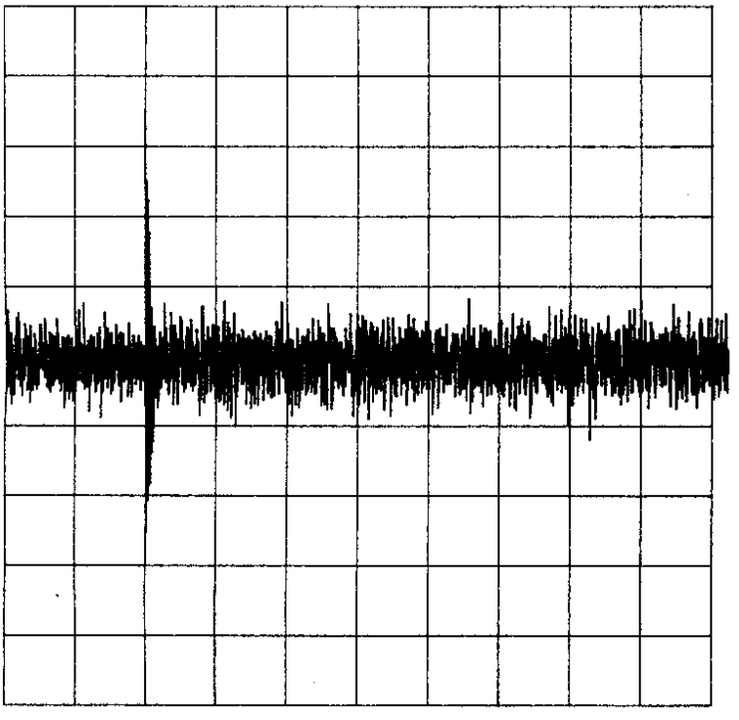

. REGO A~ 635mV T: 2ms REC AC
. B: 1 V D: - 2DIV / A

Fig. 8 beam damping, feedback loop closed.

09: 56: 05 86 Dec 05

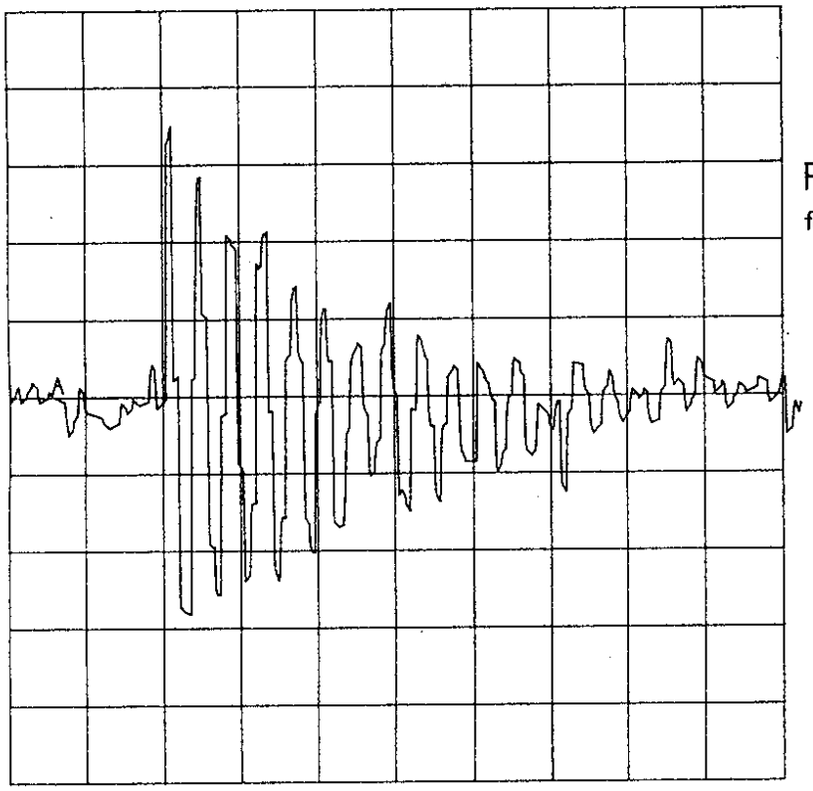

. REGO A~ 635mV T: 100us REC AC
B: 1 V D: - 2DIV / A

Fig. 9 beam damping, feedback loop closed.

09: 58: 02 86 Dec 05

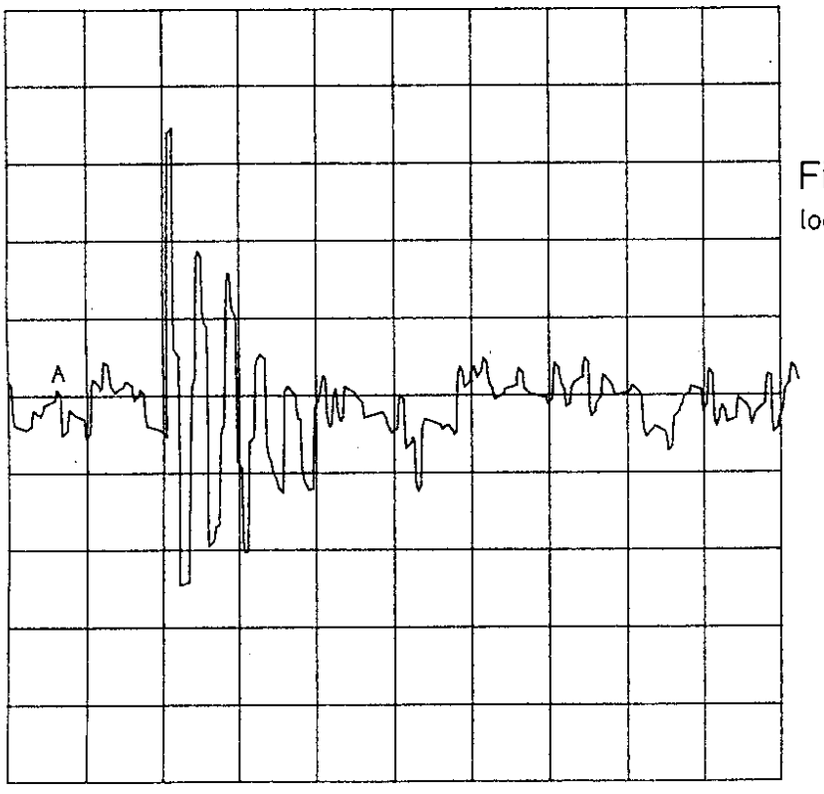

. REGO A~ 635mV T: 100us REC AC
B: 1 V D: - 2DIV / A

Fig. 10 beam damping, feedback loop closed maximum gain.